Research in Astronomy and Astrophysics, 25:075004 (7pp), 2025 July

https://doi.org/10.1088/1674-4527/addc1c
CSTR: 32081.14.RAA.addc1c

Design and Analysis of a Comprehensive Pointing Model for the Altazimuth Telescope

Hui Kong[1,2,3], Jin Xu[1,2,4], Shi-Hai Yang[1,2], Yun Li[1,2], and Zhong-Yu Yue[1,2]
[1] Nanjing Institute of Astronomical Optics & Technology, Chinese Academy of Sciences, Nanjing 210042, China; konghui23@mails.ucas.ac.cn, jxu@niaot.ac.cn
[2] CAS Key Laboratory of Astronomical Optics & Technology, Nanjing Institute of Astronomical Optics & Technology, Nanjing 210042, China
[3] University of Chinese Academy of Sciences, Beijing 100049, China
Received 2025 February 21; revised 2025 May 8; accepted 2025 May 20; published 2025 June 10

Abstract

To further improve the pointing accuracy of altazimuth telescopes, this study takes the NAOC 2.5 m telescope as the research object and develops a comprehensive pointing model. The paper first analyzes the causes of errors and accordingly constructs three core models: the basic parametric model, the spherical harmonic model, and the polynomial regression model. Among them, the basic parametric model aims to fit error terms with clear physical meanings, but its correction capability is limited and cannot fully cover all influencing factors. To address this limitation, a spherical harmonic model is introduced. This model demonstrates excellent performance in handling higher-order error terms and can accurately fit errors across the celestial sphere. Additionally, a polynomial regression model is designed to improve the fitting capability and prediction accuracy for nonlinear errors by flexibly adjusting the polynomial order. The resulting comprehensive pointing model combines the advantages of these three models, enabling more precise and complete correction of pointing errors while balancing computational complexity and accuracy by adjusting the fitting weight of each model. Experimental verification shows that the telescope's pointing accuracy is improved from 17.″805 to 3.″1029, meeting the requirements for high-precision astronomical observations.

Key words: miscellaneous – telescopes – methods: observational – methods: analytical

1. Introduction

The pointing accuracy of contemporary large-aperture telescopes has emerged as a critical technical indicator limiting cutting-edge astronomical observations. The primary strategies for enhancing telescope tracking precision involve: reducing the pointing and tracking errors of the control system itself, optimizing the precision of pointing models, and implementing guide star correction systems (Li et al. 2024). This paper primarily discusses methods for improving the accuracy of telescope pointing models, as well as the development and optimization techniques for static pointing models.

Telescope pointing models can take various forms depending on different telescope structures and application scenarios. In addition to the relatively classic basic parametric model and spherical harmonic function model, there are also other models derived from these classical ones. These include the turntable model (Zhao 2006) obtained through further analysis of mount errors based on the basic parametric model, and the optical-assisted pointing model (Sun et al. 2023) implemented by installing small optical telescope systems on radio telescopes, among others.

Zhao et al. (2023) focused on the pointing error issue of altazimuth telescopes and proposed a simplified pointing model establishment method based on two-dimensional surface fitting. This method aims to improve telescope accuracy under different observation conditions, with particular validation of its application effectiveness on the Planetary Atmospheric Spectroscopic Telescope (PAST). After calibration, the root mean square error (RMSE) of PAST's azimuth and altitude axes reached 6.″8 and 3.″8 respectively. The successful application of this model on PAST demonstrates that it achieves fast and high-precision telescope pointing calibration, making it widely applicable to pointing calibration of other altazimuth telescopes to improve observation efficiency.

Zheng et al. (2003) addressed the 1.2 m altazimuth telescope at Yunnan Observatories by proposing an all-sky pointing model to correct telescope pointing errors. They used spherical harmonic functions to fit observation data from uniformly distributed stars across the entire sky, obtaining a reasonable pointing correction function. By employing fixed-point observation methods and separation analysis of systematic and random errors, they not only improved the telescope's pointing accuracy to the arcsecond level but also introduced a small-period model for angle-measuring encoders, further enhancing image acquisition accuracy and local pointing precision.

[4] Author to whom any correspondence should be addressed.

Zhang & Wu (2001) investigated the correction of static pointing errors in altazimuth telescopes by examining both spherical harmonic and basic parametric models. Their analysis compared the advantages and disadvantages of each approach, demonstrating that the basic parametric model has fewer parameters, lower parameter correlation, and greater model stability compared to the spherical harmonic model.

Zhang (2010) tackled pointing errors in altazimuth theodolites caused by factors such as mechanical machining and imprecise alignment during actual observations. By establishing a spherical harmonic model, they proposed a new pointing error correction solution. The specific method included: observing 45 uniformly distributed stars across the sky to obtain line-of-sight deviations in the longitude and latitude directions of the theodolite, expanding the pointing errors into Fourier series using spherical harmonic functions with fourth-order zonal terms retained for simplification, and then determining spherical harmonic coefficients through least-squares fitting of observation data to correct the errors. After correction, the errors in longitude and latitude decreased from $40.''91$ and $30.''93$ to $2.''59$ and $2.''46$ respectively, with the total error reduced from $51.''29$ to $3.''57$. This method significantly enhances the pointing accuracy and reliability of theodolites, making it particularly suitable for high-precision measurement fields such as spacecraft orbit determination and planetary tracking.

2. Error Source Analysis

The sources of error in altazimuth telescopes stem from multiple factors that primarily degrade pointing accuracy and tracking performance. The following are some major error sources:

(1) Mechanical structure errors
   (a) The horizontal axis is not orthogonal to the azimuth axis.
   (b) The telescope undergoes mechanical deformation under mechanical action.
   (c) Bearing friction.
(2) Environmental factor errors
   (a) Temperature changes cause expansion and contraction of the telescope tube, bracket, and other parts.
   (b) Wind disturbances the horizontal and azimuth axes of the telescope.
   (c) Atmospheric perturbation.
(3) Instrumental errors
   (a) Encoder precision.
   (b) The telescope's optical system suffers from aberrations, distortions, and other problems.
(4) Human operational errors

3. Analysis of Telescope Pointing Models

The study employs two classical models—the basic parametric model and spherical harmonic function model—as the core framework, while innovatively incorporating a polynomial regression model for telescope pointing correction. The basic parametric model establishes its framework by selecting physical parameters closely related to telescope pointing accuracy, such as angular errors and optical axis deviations. This approach maintains clear physical interpretability while keeping computational processes relatively simple. The spherical harmonic function model achieves effective fitting of higher-order error terms by expanding errors into Fourier series, demonstrating particular efficacy in handling complex error distributions. Compared with the basic parametric and spherical harmonic function models, the polynomial regression model's greatest advantage lies in its universality (Gao et al. 2010). Its functionality includes the processing of continuous data sets and, through necessary transformations, the handling of discrete data sets. By incorporating higher-order terms of variables, it can fit data distributions of various shapes, including nonlinear relationships. Through adjustment of polynomial order, this model can adapt to different levels of data complexity and fitting requirements.

3.1. Basic Parameter Model

The study selects several key parameters that significantly impact altazimuth telescope pointing accuracy to establish the basic parameter model. These parameters typically include:

(1) Zero-point error in azimuth:

$$\Delta A = -IA$$

(2) Zero-point error in elevation:

$$\Delta E = IE$$

(3) Non-orthogonality between azimuth and pitch axes:

$$\Delta A = -NPAE \cdot \tan E$$

(4) Non-orthogonality between tube and pitch axes:

$$\Delta A = -CA \cdot \sec E$$

(5) Tilt of azimuth axis in a north–south direction:

$$\Delta A = -AN \cdot \sin A \cdot \tan E,\ \Delta E = -AN \cdot \cos A$$

(6) Tilt of azimuth axis in an east–west direction:

$$\Delta A = -AW \cdot \cos A \cdot \tan E,\ \Delta E = AW \cdot \sin A$$

(7) Flexure of the tube:

$$\Delta E = -TX \cdot \tan(90^\circ - E)$$

Since all these parameters have clear physical meanings and are relatively easy to calculate, a basic parameter model can be established based on them. Among them, ΔA, ΔE represent the pointing errors in azimuth (AZ) and elevation (ALT)

respectively, while A and E are the actual azimuth angle and pitch angle.

$$\Delta A = -IA - NPAE \cdot \tan E - CA \cdot \frac{1}{\cos E} - AN \cdot \sin A \cdot \tan E - AW \cdot \cos A \cdot \tan E \quad (1)$$

$$\Delta E = IE - AN \cdot \cos A + AW \cdot \sin A - TX \cdot \tan(90^\circ - E) \quad (2)$$

By fitting function coefficients, you can obtain the basic parameter correction model for the telescope.

3.2. Spherical Harmonic Function Model

Spherical harmonics are functions defined on a sphere, suitable for describing the error distribution on a sphere or hemisphere. In telescope pointing error correction, the spherical harmonics model applies to telescopes of various frame structure and can fit spherical complex error. In the spherical coordinate system, γ is the radical distance, θ is the polar angle, and ϕ is the azimuthal angle, the form of the Laplace equation is:

$$\nabla^2 \Psi(\gamma, \theta, \phi) = 0$$

Among them, ∇^2 represents the Laplacian operator, which is expressed as follows in spherical coordinates:

$$\nabla^2 = \frac{1}{\gamma^2}\frac{\partial}{\partial \gamma}\left(\gamma^2 \frac{\partial}{\partial \gamma}\right) + \frac{1}{\gamma^2 \sin\theta}\frac{\partial}{\partial \theta}\left(\sin\theta \frac{\partial}{\partial \theta}\right) + \frac{1}{\gamma^2 (\sin\theta)^2}\frac{\partial^2}{\partial \phi^2}$$

Using the method of separation of variables, the above equation can be solved. Let $\Psi(\gamma, \theta, \phi)$ be decomposed into the product of the radial part $\Gamma(\gamma)$, the polar angle part $\Theta(\theta)$, and the azimuthal angle part $\Phi(\phi)$:

$$\Psi(\gamma, \theta, \phi) = \Gamma(\gamma)\Theta(\theta)\Phi(\phi) \quad (3)$$

3.3. Polynomial Regression Model

The polynomial regression model is an extension of linear regression. Linear regression uses a straight line to fit data, such as a linear function $y = kx + b$, while polynomial regression uses curves to fit the data, such as a quadratic function $y = ax^2 + bx + c$, a cubic function $y = ax^3 + bx^2 + cx + d$, and higher-order functions to fit the data. We now present the polynomial regression model using a 5th-order bivariate function as an illustrative case. Here, β_0, …, β_{20} represent the coefficients obtained through model training, where x_1 and x_2 denote the input variables, and y is the output.

$$\begin{aligned} y = {} & \beta_0 + \beta_1 x_1 + \beta_2 x_2 + \beta_3 x_1^2 + \beta_4 x_1 x_2 \\ & + \beta_5 x_2^2 + \beta_6 x_1^3 + \beta_7 x_1^2 x_2 \\ & + \beta_8 x_1 x_2^2 + \beta_9 x_2^3 + \beta_{10} x_1^4 + \beta_{11} x_1^3 x_2 \\ & + \beta_{12} x_1^2 x_2^2 + \beta_{13} x_1 x_2^3 + \beta_{14} x_2^4 \\ & + \beta_{15} x_1^5 + \beta_{16} x_1^4 x_2 + \beta_{17} x_1^3 x_2^2 \\ & + \beta_{18} x_1^2 x_2^3 + \beta_{19} x_1 x_2^4 + \beta_{20} x_2^5 \end{aligned} \quad (4)$$

4. Model Evaluation Metrics

In the process of developing a telescope pointing model, evaluation metrics serve as critical tools for optimizing model performance, verifying effectiveness, and ensuring practical utility. Currently adopted evaluation metrics include mean absolute error, RMSE, mean absolute percentage error, coefficient of determination (R^2), and sum of squared errors (SSE; Wang et al. 2023). The study evaluates the model's fitting performance by calculating RMSE and R^2, using cross-validation to prevent overfitting in the proposed polynomial model.

4.1. Root Mean Square Error and Fitting Goodness

Root mean square error is a statistical metric that quantifies the deviation between the model's predicted pointing positions and actual observed positions, reflecting the overall accuracy of the model. For high-precision astronomical observations, RMSE must be below $5''$. Goodness of fit is an indicator that measures the degree of agreement between the model's predicted values and actual observational data, assessing whether the model captures the physical principles governing telescope pointing errors. There are various calculation methods for goodness of fit, with the most common being the coefficient of determination, also known as the goodness-of-fit coefficient. Its value ranges between 0 and 1, where values closer to 1 indicate better model fitting. Assuming that there are n sets of observation data, each with a corresponding predicted value, the formula for calculating the RMSE is:

$$\mathrm{RMSE} = \sqrt{\frac{1}{n}\sum_{i=1}^{n}(\hat{y}_i - y_i)^2} \quad (5)$$

The calculation formula of the goodness-of-fit coefficient R^2 is as follows:

$$R^2 = 1 - \frac{\sum_{i=1}^{n}(y_i - \hat{y}_i)^2}{\sum_{i=1}^{n}(y_i - \bar{y}i)^2} \quad (6)$$

Among them, y_i is the actual value of the observed data for group i, $\hat{y}_i$ is the predicted value of the observed data for group i, and $\bar{y}_i$ is the average value of all observed data. In the design, RMSE is first used to assess the overall fitting effect of the model. When RMSE meets the requirements, R^2 is used to

verify the model's ability to fit the overall trend. Since RMSE averages the squared residuals, even if most data points fit well while a subset exhibits significant deviations, the errors are uniformly distributed, leading to an artificially reduced RMSE. If the new data is in the part where the fitting result is not good, the fitting result will have a huge deviation. Therefore, R^2 is added to test the fitting trend.

4.2. Cross-validation

Although higher-order polynomial fitting can achieve better fitting results, the model may capture noise and lead to overfitting-performing well on the training set but poorly on new data. Therefore, cross-validation is employed to optimize the division of training and test sets, enhancing the model's generalization capability. Cross-validation involves partitioning the dataset into K mutually exclusive subsets. Each iteration uses $K - 1$ subsets for training and one subset for validation. After each training round, error metrics are computed. After K rounds of calculation, the optimal polynomial order is determined by synthesizing the K results, and the final model is trained using the full dataset. Compared to a single train-test split, this approach reduces sensitivity to data partitioning, effectively mitigating overfitting and underfitting issues caused by arbitrary splits.

5. Comprehensive Pointing Model

The basic parameter model, spherical harmonic model, and polynomial regression model each has distinct advantages but also certain limitations. The basic parametric model struggles to comprehensively account for complex error sources, particularly when dealing with nonlinear or higher-order errors, resulting in limited correction accuracy. Spherical harmonics, being global basis functions, exhibit weaker modeling capabilities for localized systematic errors. Direct polynomial correction may lead to overfitting if the polynomial order is excessively high. Therefore, the form of the integrated pointing model is determined as a combination of the basic parametric-spherical harmonic model and the polynomial regression model. The primary parameters of this model retain clear physical significance, while the additional parameters enable the model to handle complex spherical errors and nonlinear errors.

5.1. Design of Comprehensive Directional Model

Before model training, sample quality is first evaluated to prevent unreasonable samples from affecting model accuracy and causing overfitting (Zhang et al. 2023). Subsequently, the basic parametric-spherical harmonic model is employed for fitting to derive the telescope's pointing error correction model. The residuals are obtained by subtracting the model-predicted pointing errors from the actual pointing errors. The

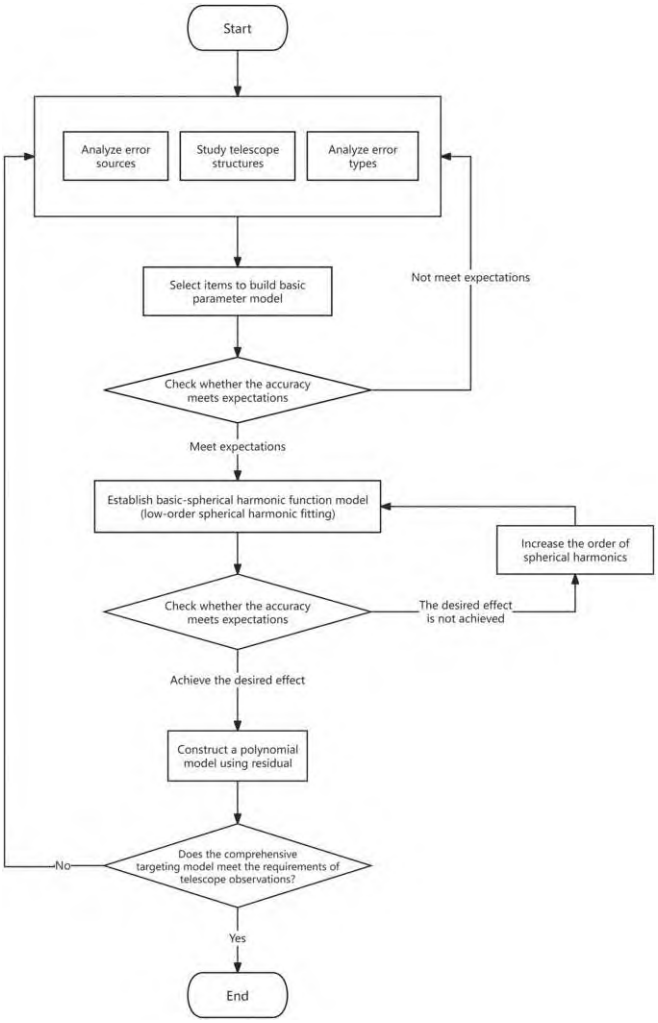

Figure 1. The process of creating the comprehensive pointing model.

polynomial regression model is then applied for further fitting. Its input consists of a feature matrix formed by actual azimuth angles and their corresponding actual elevation angles, while its output targets the residuals remaining after the basic parametric-spherical harmonic model fitting. These residuals represent the objectives for the polynomial regression model to fit.

The process of establishing the comprehensive pointing model is shown in Figure 1, and the specific process of building the polynomial regression model is illustrated in Figure 2.

To identify the optimal polynomial model, polynomial fitting from 1st to 15th order is performed. During fitting, the dataset is divided into five mutually exclusive subsets for cross-validation. Each polynomial order undergoes five rounds of training and validation. In each round, four subsets are used for training while the remaining subset serves as the validation set. After fitting, errors are computed to obtain RMSE and R^2

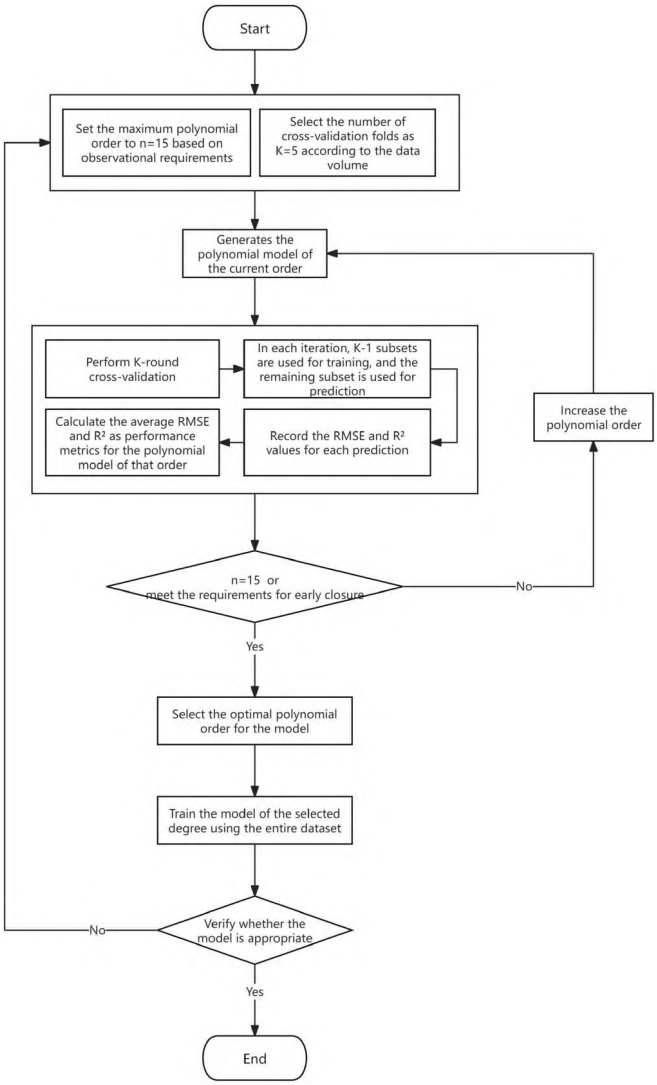

Figure 2. The process of making a polynomial regression model.

values for each polynomial order across all five folds. The average RMSE and R^2 from the five cross-validation rounds serve as comprehensive performance metrics for each polynomial order. The training process terminates after evaluating all 15 polynomial orders, or when further increases in order no longer improve scores. The fitting accuracies for different polynomial orders are presented in Table 1.

By comparing the average RMSE and R^2 of models with different polynomial orders, the optimal order for the polynomial regression model is determined to be 5. Subsequently, the entire dataset is used to train and obtain the final model. The residuals are then calculated based on this model and added to the fitting results from the basic parametric-spherical harmonic model to yield more accurate pointing errors. The integrated pointing model combining all three

Table 1
Comparison of Polynomial Fitting Accuracy of Different Orders

Polynomial Order	RMSE	AZ_R^2	ALT_R^2
1	3.521	0.951	0.956
2	3.528	0.957	0.961
3	3.504	0.960	0.981
4	3.334	0.954	0.980
5	3.177	0.954	0.990
6	6.999	1.045	0.936
7	6.888	1.931	1.070
8	10.804	2.449	1.131

approaches is presented as follows:

$$\begin{aligned}\Delta A_{b-s} = &-a_0 - a_1\tan E - a_2\frac{1}{\cos E} - a_3\sin A\tan E\\ &- a_4\cos A\tan E + a_5\frac{1}{\cos E} + a_6\frac{\sin E}{\cos E}\\ &+ a_7\cos A + a_8\sin A + a_9\frac{sin^2E}{\cos E}\\ &+ a_{10}\cos A\sin E + a_{11}\sin A\sin E + a_{12}\frac{\sin^3 E}{\cos E}\\ &+ a_{13}\cos A\sin^2 E + a_{14}\sin A\sin^2 E + a_{15}\frac{sin^4E}{\cos E}\\ &+ a_{16}\cos A\sin^3 E + a_{17}\sin A\sin^3 E\end{aligned} \tag{7}$$

$$\begin{aligned}\Delta E_{b-s} = &\, e_0 - e_1\cos A + e_2\sin A - e_3\tan(90^\circ - E)\\ &+ e_4 + e_5\sin A + e_6\cos A\\ &+ e_7\sin E + e_8\cos E + e_9\cos A\sin E\\ &+ e_{10}\cos A\sin^2 E + e_{11}\cos^3 A\end{aligned} \tag{8}$$

$$\begin{aligned}residual\_error = &\,\beta_0 + \beta_1 A + \beta_2 E + \beta_3 A^2 + \beta_4 AE\\ &+ \beta_5 E^2 + \beta_6 A^3 + \beta_7 A^2 E + \beta_8 AE^2\\ &+ \beta_9\quad E^3 + \beta_{10}A^4 + \beta_{11}A^3E + \beta_{12}A^2E^2\\ &+ \beta_{13}AE^3\\ &+ \beta_{14}E^4 + \beta_{15}A^5\\ &+ \beta_{16}A^4E + \beta_{17}A^3E^2\\ &+ \beta_{18}A^2E^3 + \beta_{19}AE^4 + \beta_{20}E^5\end{aligned} \tag{9}$$

$$\Delta A = A + residual\_error_A \tag{10}$$

$$\Delta E = E + residual\_error_E \tag{11}$$

Among them, ΔA_{b-s} and ΔE_{b-s} are the pointing errors of the azimuth and elevation directions calculated by the spherical harmonic function model. A is the actual azimuth, E is the actual pitch angle, a_0, ..., a_{17}, e_0, ..., e_{11} are the coefficients to be fitted and residual_error is the residual obtained from fitting the polynomial regression model, ΔA and ΔE are more accurate pointing errors in the azimuth and elevation directions after correction by the comprehensive pointing model. By

Table 2
Composite Points to the Fit Factor of the Model

ΔA				ΔE			
Basic Parameters + Spherical Harmonics		Polynomial		Basic Parameters + Spherical Harmonics		Polynomial	
a_0	0.01734881	β_0	0	e_0	289.4781944	β_0	0
a_1	−504.011236	β_1	−0.00038691	e_1	−33.55263763	β_1	0.00105668
a_2	388.651726	β_2	0.00148707	e_2	−0.00067162	β_2	0.00105836
a_3	0.00275147	β_3	−0.00355569	e_3	−0.00798313	β_3	0.00014366
a_4	−0.00347962	β_4	0.00102788	e_4	−0.00798311	β_4	−0.00027569
a_5	388.6240869	β_5	−0.00088658	e_5	33.54947599	β_5	−0.00013176
a_6	−503.7356211	β_6	0.00039235	e_6	175.8212464	β_6	−0.00163951
a_7	0.02156474	β_7	−0.00224617	e_7	0.01924074	β_7	0.00024733
a_8	−0.01392081	β_8	0.00110034	e_8	0.00317804	β_8	−0.00029106
a_9	−0.66293641	β_9	−0.00200213	e_9	−0.00003223	β_9	−0.00192128
a_{10}	−0.12695353	β_{10}	0.00142803	e_{10}	113.6553971	β_{10}	−0.00002583
a_{11}	0.08586931	β_{11}	−0.00056701	e_{11}	113.6556929	β_{11}	0.00024688
a_{12}	0.67186181	β_{12}	0.00059864			β_{12}	−0.00002627
a_{13}	0.23401295	β_{13}	−0.0002576			β_{13}	−0.00008167
a_{14}	−0.15937291	β_{14}	0.00037958			β_{14}	0.00007223
a_{15}	−0.25662396	β_{15}	−0.00004696			β_{15}	0.00051163
a_{16}	−0.1343298	β_{16}	0.00102432			β_{16}	−0.000074
a_{17}	0.09432191	β_{17}	−0.00064706			β_{17}	−0.00001214
		β_{18}	0.0002614			β_{18}	−0.00007652
		β_{19}	−0.000206			β_{19}	0.00014522
		β_{20}	0.00071152			β_{20}	0.00067667

substituting measured values, the least squares method is used to fit Equations (7) and (8) to obtain the coefficients of the error correction function for the basic parametric-spherical harmonic model. Then, Equation (9) is fitted to derive the coefficients of the polynomial regression model. The final fitting coefficients of the integrated pointing model are presented in Table 2.

5.2. Comparison of Model Fitting Effect

In order to compare the fitting effect of different pointing models, this paper adopts the method of measurement and verification, observes the evenly distributed stars in the sky, and inputs pointing commands to the telescope according to the azimuth interval of about 30° and the elevation interval of about 10°, and the azimuth and elevation angles of the telescope are saved as the actual values. A total of 76 sets of star maps were taken, and the R.A. and decl. corresponding to the center of the 76 sets of images were obtained by comparing them with the standard star maps. Then, according to the shooting time, the geographic latitude and longitude of the observation site, the altitude, the air pressure and the air temperature, the R.A. and decl. are converted into the azimuth and elevation angles in the horizon coordinate system, that is, the theoretical azimuth angle and the theoretical elevation angle. The combined model of three core models and any two models and the comprehensive pointing model were used for fitting, and the fitting effect (unit: arcseconds) is shown in Table 3.

Table 3
Comparison of Model Fitting Effects

Pointing Model	RMSE	AZ_R^2	ALT_R^2
Basic Parametric Model	4.4996	0.9311	0.9536
Spherical Harmonic Function Model	4.8258	0.8833	0.9649
Polynomial Regression Models	3.3851	0.9537	0.9677
Spherical Harmonic Function + Polynomial Regression	3.1832	0.9595	0.9647
Basic Parametric + Polynomial Regression	3.4325	0.9583	0.966
Basic Parametric + Spherical Harmonic	3.4979	0.9447	0.9654
Basic Parametric + Spherical Harmonic + Polynomial Regression	3.1029	0.9742	0.9799

6. Experimental Analysis

Comparing the three core models, it is found that the polynomial regression model has better RMSE and R^2 than the other two models, showing the best fitting performance. The basic parametric model comes second, while the spherical harmonic function model shows poorer overall fitting due to its inadequate fitting in the azimuth direction. Comparing any two-model combinations, it is found that both the basic parametric model and spherical harmonic function model show improved RMSE and R^2 after incorporating polynomials. Moreover, the combination of spherical harmonic function

Figure 3. Comparison of the actual error of AZ with the fitting results.

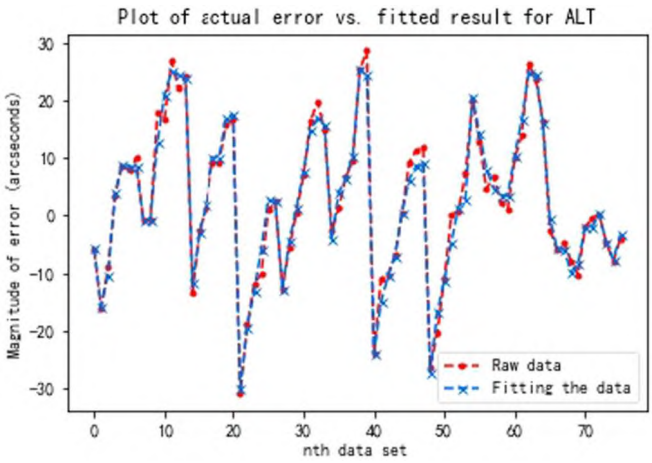

Figure 4. Comparison of the actual error of ALT with the fitting results.

with polynomials demonstrates better fitting performance than using polynomials alone.

The integrated pointing model achieves the best results, with RMSE reduced to $3\overset{''}{.}1029$, indicating good fitting for most data points. The R^2 values for AZ and ALT reach 0.9742 and 0.9799, respectively, proving that the model captures the overall trend well without any abnormal fitting sections. Figures 3 and 4 visually present the fitting performance of the integrated pointing model, where the horizontal axis represents the sequence numbers of observation data, and the vertical axis shows the magnitude of pointing errors. The left plot displays comparison curves between actual errors and model fitting results in the AZ direction. The plot shows consistent overall trends between raw data and fitted data, particularly in regions with large fluctuations where the two curves largely coincide. The right plot shows comparison curves for the ALT direction. Most regions also demonstrate good fitting between raw data and fitted data, with the two curves closely following each other in overall trend. From both plots, the model effectively captures the overall trends in both AZ and ALT directions.

7. Conclusions and Prospects

The basic parametric model provides a concise framework for rapid pointing error description, the spherical harmonic model specializes in spherical error correction, and the polynomial model adapts its order to resolve nonlinear errors. By combining these three approaches, the model preserves physical interpretability while achieving high flexibility and accuracy. Ultimately, the pointing accuracy of the NAOC 2.5 m telescope achieved a pointing accuracy improvement from $17\overset{''}{.}805$ to $3\overset{''}{.}1029$. Compared to existing studies, the integrated pointing model can balance computational complexity and precision by appropriately adjusting each model's parameters and fitting weights under different requirements and constraints. It not only significantly enhances the accuracy and robustness of the telescope pointing system but also comprehensively considers various error sources, improving the model's adaptability and precision. This multi-level, multi-dimensional error fitting method holds a high practical value in telescope pointing control systems.

Although the integrated pointing model limits the fitting order and weight of each sub-model, it still involves numerous parameters and relatively complex computations. This may create computational bottlenecks for real-time or near-real-time telescope pointing control systems. Therefore, it is primarily used for the development and optimization of static pointing models. Future work will focus on further optimizing the algorithm to improve coordination between sub-models and eliminate redundancy, thereby reducing complexity while maintaining high precision and computational efficiency. Additionally, research will continue on the development and optimization of dynamic pointing models.

References

Gao, Z. M., Zhao, J., & He, S. P. 2010, CNS, 2, 308
Li, Y., Ye, Y., Yang, S. H., et al. 2024, RAA, 24, 035004
Sun, Z. X., Mao, Y. D., Wang, J. Q., et al. 2023, AcASn, 64, 3
Wang, W. J., Han, B. Q., Wang, L. Y., et al. 2023, RAA, 23, 095003
Zhang, W. B. 2010, Ome Information, 27, 48
Zhang, X. X., & Wu, L. D. 2001, AcASn, 2, 198
Zhang, Z. H., Ye, Q., Fu, L., et al. 2023, RAA, 23, 015001
Zhao, J. 2006, Research on Improving the Pointing Accuracy of Satellite Laser Ranging Telescope at Changchun Satellite Station[D]. Changchun University of Science and Technology
Zhao, Y., Wang, Y., He, F., et al. 2023, ApSci, 13, 11238
Zheng, X. M., Wang, W., Zhang, Y. C., & Feng, H. S. 2003, AcASn, 3, 330